

LEP Higgs physics revisited

DESY Summer Student project

Julia Gehrlein^{a, 1}

Supervisors: Emanuele Bagnaschi, Georg Weiglein

^a *Institut für Theoretische Teilchenphysik, Karlsruhe Institute of Technology,
Engesserstraße 7, D-76131 Karlsruhe, Germany*



Abstract

In this summer student project we investigate the expected signal and background events for Higgs production at LEP as well as the expected limits of the coupling of the Higgs boson to the Z boson in the light of an additional light Higgs boson. The Higgs production via W boson fusion and the Higgs production in Higgsstrahlung with a subsequent decay of the Z boson to a fermion-antifermion pair are the most relevant process for Higgs production at LEP energies of ≈ 200 GeV. The expected number of produced Higgs boson is ≈ 4 at LEP at $\sqrt{s} = 206.5$ GeV.

¹E-mail: julia.gehrlein@student.kit.edu

1 Introduction

The discovery of a Higgs boson by CMS [1] and ATLAS [2] represented a milestone in the confirmation in the Standard Model (SM) of Particle physics. The existence of a Higgs particle ensures unitarity in the scattering of longitudinal polarized W bosons and allows the introduction of particle masses without breaking the gauge symmetry of the theory via the Higgs mechanism. The underlying idea of this mechanism is the introduction of a complex scalar field into the theory whose ground state acquires a non-zero value (vacuum expectation value VEV) v . The potential of the Higgs field does not share anymore the same symmetry as the full Lagrangian of the theory and hence the symmetry is spontaneously broken by the VEV of the Higgs field. Due to the Goldstone theorem which implies that a spontaneously broken local symmetry leads to massless Goldstone bosons whose degrees of freedom are then eaten up by the gauge bosons only one degree of freedom of the Higgs field remains as a physical particle in the theory. This is the Higgs boson whose mass is a free parameter in the theory. The gauge bosons become massive via the interaction with the Higgs field after the spontaneous symmetry breaking, ie. after the Higgs field acquired its VEV. The gauge boson masses are proportional to the VEV of the Higgs field [3]

$$m_W^2 = \frac{g^2 v^2}{4}, m_Z^2 = \frac{(g^2 + g'^2) v^2}{4}, \quad (1.1)$$

where g is the gauge coupling of the $SU(2)_L$ and g' is the gauge coupling of the $U(1)_Y$.

The fermion masses are generated via the Yukawa interaction with the Higgs field Φ after spontaneous symmetry breaking $-y_{ij} \bar{f}_{Li} \Phi f_{Rj}$ where y_{ij} is a 3×3 matrix containing the Yukawa interactions of the fermions and f_L stands for the $SU(2)_L$ quark or lepton doublets and f_R for the $SU(2)_L$ quark or lepton singlets.

In 2012 a SM-like Higgs boson with a mass of 125 GeV boson was discovered. The properties of the discovered particle are compatible with the SM predictions. Also the couplings to the fermions and gauge bosons are to some precision in accordance with the theory predictions [1, 2].

Before 2012 only lower bounds on the Higgs mass were achieved by the previous colliders for example LEP set the lower limit $m_H > 114.4$ GeV [4]. The LEP collider operated between 1989 and 2000 and was an electron positron ring-collider with four interaction regions which were instrumented with the detectors L3, ALEPH, OPAL and DELPHI. Until 1995 the accelerator operated at the Z boson resonance to perform electroweak precision measurements, afterwards the center of mass energy was increased to 209 GeV [5].

In this project we investigate the expected signal and background events for Higgs production at LEP as well as the expected limits of the coupling of the Higgs boson to the Z boson in the light of an additional light Higgs boson.

2 The Higgs boson production and decay channels

In this section we analyse the Higgs boson production channels relevant at LEP before we investigate the expected signal and background events taking the decays of the Higgs boson into account.

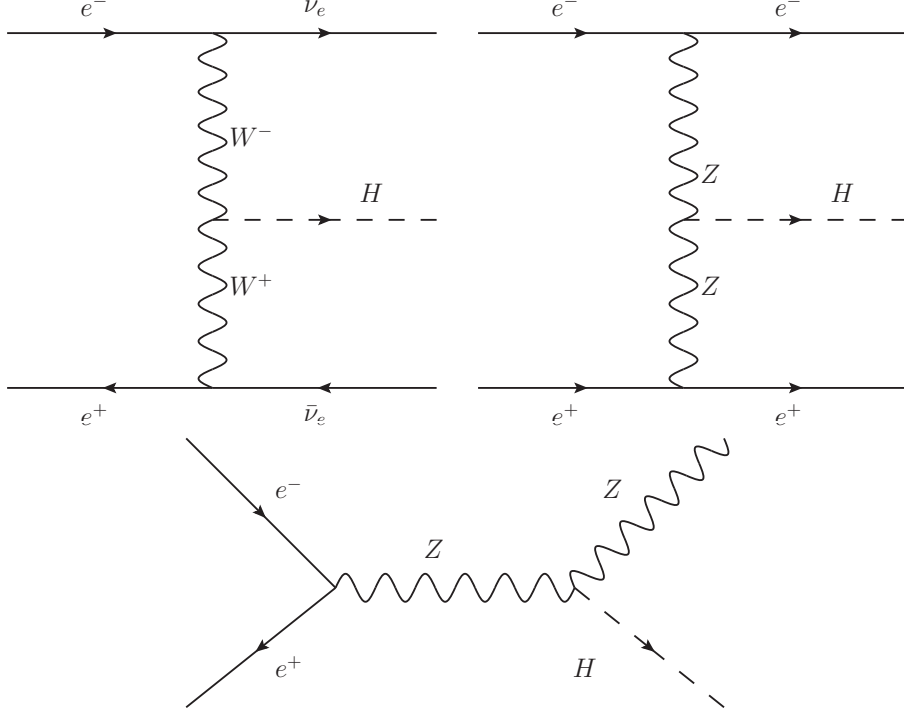


Figure 1: Feynman diagrams for Higgsstrahlung and vector boson fusion.

2.1 The Higgs production channels at LEP

The primary production channels of the Higgs boson at electron-positron colliders like LEP are $e^+ + e^- \rightarrow Z + H$ (Higgsstrahlung) and $e^+ + e^- \rightarrow \bar{\nu}_e + \nu_e + W^* + W^* \rightarrow \bar{\nu}_e + \nu_e + H$ (W-boson fusion) [3]. Higgsstrahlung is dominant at low energies since vector boson fusion involves three weak vertices and is hence suppressed by $\mathcal{O}(\alpha_w)$, see Fig. 1. The corresponding cross sections for the production processes are given as in ref. [6]

$$\sigma(e^+e^- \rightarrow HZ) = \frac{g_{ZZH}^2}{4\pi} \frac{G_F(v_e^2 + a_e^2)}{96\sqrt{2}s} \beta_{HZ} \frac{\beta_{HZ}^2 + 12M_Z^2/s}{(1 - M_Z^2/s)^2}, \quad (2.1)$$

where $\beta_{ij}^2 = [1 - (M_i + M_j)^2/s]$, $v_e = -1 + 4\sin^2\theta_W$ and $a_e = -1$ and [7]

$$\sigma(e^+e^- \rightarrow H\nu_e\bar{\nu}_e) = \frac{G_F^3 m_W^4}{4\sqrt{2}\pi^3} \int_{x_H}^1 dx \int_x^1 \frac{dy F(x,y)}{[1 + (y-x)/x_W]^2} \quad (2.2)$$

with $F(x,y) = \left(\frac{2x}{y^3} - \frac{1+3x}{y^2} + \frac{2+x}{y} - 1\right) \left[\frac{z}{1+z} - \log(1+z)\right] + \frac{x}{y^3} \frac{z^2(1-y)}{1+z}$ and $x_H = m_H^2/s$, $x_W = m_W^2/s$, $z = y(x - x_H)/(xx_W)$.

With an increasing center of mass energy \sqrt{s} the cross section for the Higgsstrahlung is decreasing as s^{-1} whereas the cross section for W boson fusion is increasing as $\ln(s/m_H^2)$. Hence Higgsstrahlung is dominant at low energies and W boson fusion is dominant at high energies. The cross section of Z boson fusion is suppressed by one order of magnitude compared to the one of W boson fusion. The associated production of a Higgs boson with a top quark pair $e^+ + e^- \rightarrow t\bar{t}H$ is relevant above $\sqrt{s} \approx 500$ GeV for a SM Higgs [8].

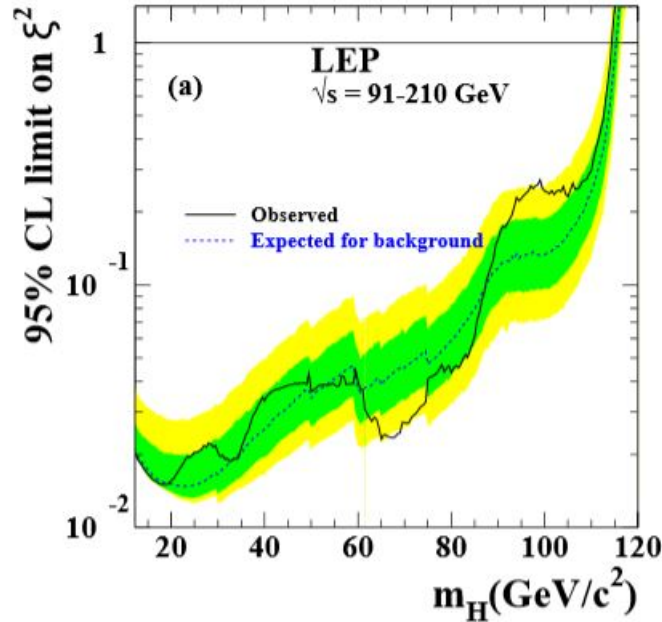


Figure 2: 95% limit of ratio of the HZ coupling compared to SM value $\xi = g_{HZZ}/g_{HZZ}^{SM}$ in dependence of the Higgs mass, taken from [4].

The production channels involve the coupling of the Higgs boson to the gauge bosons which reads in the Standard Model (SM) [3]

$$g_{HVV} = 2m_V^2/v \quad (2.3)$$

where v is the vev of the Higgs boson $v = 246$ GeV and m_V is the mass of the gauge boson $V = W$ or Z . At LEP limits on the ratio $\xi = g_{HZZ}/g_{HZZ}^{SM}$ in dependence on the Higgs mass were obtained. The result can be seen in Fig. 2.

LEP reached at the end of the run in 2000 a center of mass energy of 209 GeV [4] but only with a small luminosity, the main luminosity at energies above 200 GeV was collected at 206.5 GeV (cf. Tab.1). Since $m_Z = 91$ GeV a Higgs with a mass of 125 GeV cannot be produced in Higgsstrahlung with an on-shell Z boson.

In Fig. 3 the dependence of the cross sections on the center of mass energy for both processes are shown. The red points are the numerical results of an implementation of the processes in MadGraph [9] where 1000 events were generated with input values for the relevant masses and couplings according to the SM values. The dashed lines show the theoretical predictions for the cross sections according to eqs. (2.1, 2.2) which agree very well with the numerical results.

We see that Higgs production via Higgsstrahlung in association with an on-shell Z boson is relevant for center of mass energies above 216 GeV (which is the sum of the Higgs mass and the Z boson mass). Furthermore Higgsstrahlung is dominant at low energies as anticipated whereas the impact of W boson fusion increases with the center of mass energy. We obtain a lower bound for the center of mass energy where a Higgs boson can be produced in W boson fusion of $\sqrt{s} \gtrsim 140$ GeV.

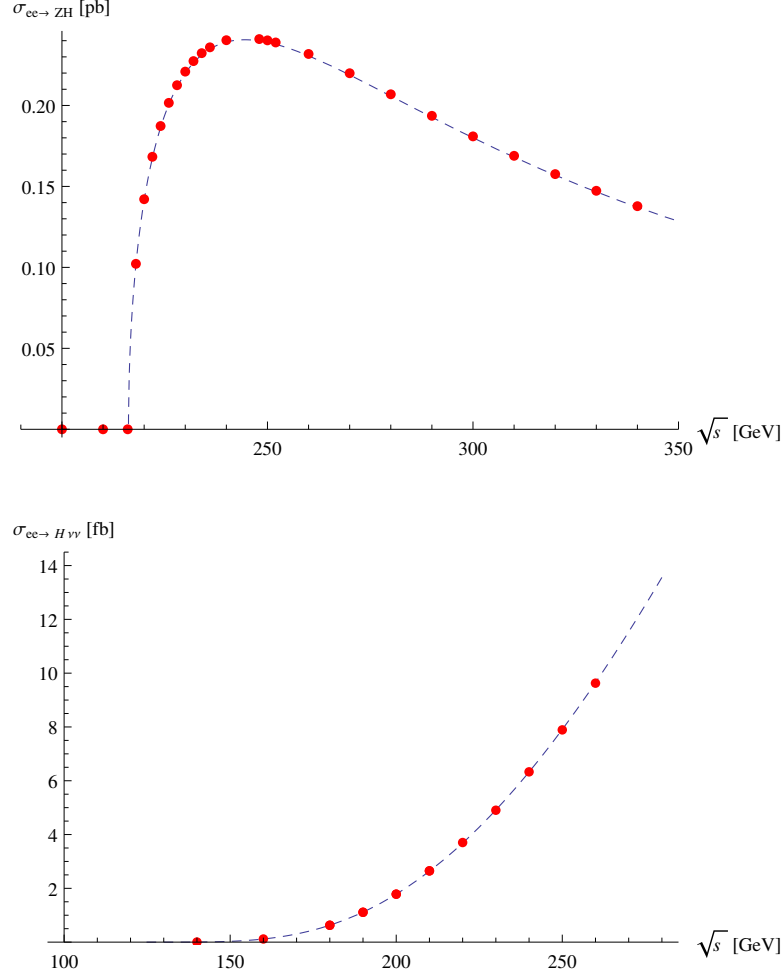


Figure 3: Cross sections for the dominant Higgs production mechanism at LEP, Higgsstrahlung (with an on shell Z boson) and W boson fusion in the SM. The red points show the results from MadGraph, the dashed lines are the theory predictions according to eqs. (2.1, 2.2) with $m_H = 125$ GeV.

\sqrt{s} [GeV]	Luminosity [pb^{-1}]
130.3	6
136.3	6
140.2	1
161.3	12
172.1	12
182.7	60
188.6	180
191.6	30
195.5	90
199.5	90
201.8	40
204.8	80
206.5	130
208.0	8
130.3-208.0	745

Table 1: The mean center of mass energy and the corresponding luminosity recorded by each experiment at LEP 2 [10]. The last row sums up the number of events and the total number of luminosity collected at LEP 2.

2.2 Results for the expected rate of events

The mean center of mass energies and the corresponding luminosity recorded by each experiment at LEP 2 are summarised in Tab. 1. In the following we will focus on the high center of mass energies above 188 GeV where the number of events is larger.

Since LEP did not reach the necessary center of mass energy to produce a Higgs boson with $m_H = 125$ GeV via Higgsstrahlung with an on shell Z boson we take the Higgs production with off shell Z bosons and their subsequent decay to a fermion-antifermion pair into account. In Tab. 2 the cross sections for the W boson fusion including the interference term from Higgsstrahlung when the Z bosons decays into electron neutrinos, the Z boson fusion including the interference term from Higgsstrahlung when the Z bosons decays into electrons and for Higgsstrahlung when the Z bosons decays into a fermion-antifermion pair are shown. As anticipated before, the cross section including the Z boson fusion is smaller than the cross section including the W boson fusion. At $\sqrt{s} \gtrsim 204$ GeV the cross section for Higgsstrahlung with the subsequent Z decay is larger than the cross section for the W boson fusion including the interference term because of the finite width of the Z boson. In Fig. 4 the cross sections for vector boson fusion (the sum of the process with W and Z bosons) including the inference with Higgsstrahlung and the cross section for Higgsstrahlung with the subsequent decay of the Z boson to fermions is shown.

The largest contribution with over 50% of the total cross section of the Higgsstrahlung process comes from the decay of the Z boson to quarks as it can be seen in Tab. 3 where the cross sections for Higgsstrahlung with the decay of the Z boson to neutrinos, quarks and charged leptons are represented.

The impact of the interference term for the W boson fusion is not negligible since it contributes more than 30% to the total cross section at $\sqrt{s} \gtrsim 200$ GeV as can be seen in Tab. 4

\sqrt{s} [GeV]	$\sigma_{VBF+interf}^{H\nu_e\bar{\nu}_e}$ [fb]	$\sigma_{VBF+interf}^{He^+e^-}$ [fb]	σ_{HS} [fb]
188.6	1.4745	0.04277	0.69558
191.6	1.7334	0.04593	0.91521
195.5	2.1108	0.04784	1.302
199.5	2.5725	0.04743	1.8967
201.8	2.8619	0.04568	2.3913
204.8	3.2969	0.0376	3.2886
206.5	3.5756	0.0308	4.0123
208.0	3.8391	0.0247	4.8702

Table 2: The cross sections for Higgs production with vector boson fusion with W bosons including the interference term with Higgsstrahlung, vector boson fusion with Z bosons including the interference term from Higgsstrahlung with a subsequent decay of the Z boson to electrons and Higgsstrahlung where the Z boson decays to fermions for different center of mass energies and $m_H = 125$ GeV.

\sqrt{s} [GeV]	$\sigma_{H,Z\rightarrow\nu_l\bar{\nu}_l}$ [fb]	$\sigma_{H,Z\rightarrow q\bar{q}}$ [fb]	$\sigma_{H,Z\rightarrow l+l-}$ [fb]	$\sigma_{HS,total}$ [fb]
188.6	0.2559	0.3776	$6.208\cdot 10^{-2}$	0.69558
191.6	0.3135	0.5117	$9.001\cdot 10^{-2}$	0.91521
195.5	0.4162	0.7466	0.1392	1.302
199.5	0.5706	1.113	0.2131	1.8967
201.8	0.6934	1.426	0.2719	2.3913
204.8	0.9152	1.989	0.3844	3.2886
206.5	1.094	2.448	0.4703	4.0123
208.0	1.293	3.008	0.5692	4.8702

Table 3: The mean center of mass energy and the corresponding cross sections for Higgsstrahlung with the subsequent decay of the Z boson to neutrinos, quarks and charged leptons with $m_H = 125$ GeV. The last columns sum up all the contributions from the decay channels.

and in Fig. 5 where the cross sections as a function of \sqrt{s} are represented.

From the results of the cross section we calculate the number of events for the Higgs production as $N = \sigma \cdot L$. The results are shown in Tab. 5. The highest number of events is $N_{total} \approx 3.95$. The sum of the total number of produced Higgs bosons between $\sqrt{s} = 188.6 - 208.0$ GeV at LEP is 11.89.

Similar estimates have been done in [11] where the authors find for $m_H = 115$ GeV $\sigma_{HS} \approx 50$ fb, $\sigma_{VBF+interf} \approx 5.5$ fb and for $m_H = 125$ GeV $\sigma_{VBF+interf} \approx 2.9$ fb, for $\sigma_{HS} \approx 4.2$ fb. Our results (cf. Tab. 6) are compatible with these numbers but exceed them for $m_H = 125$ GeV.

2.3 Dominant decay channels of the Higgs boson

Since the couplings of the Higgs boson to the fermions are proportional to the masses of the particles the dominant decay channels are the decays to the heaviest particles for which the decay is kinematically allowed. The decay $H \rightarrow t\bar{t}$ with $m_H = 125$ GeV is on shell top quarks ($m_H = 174$ GeV) is kinematically forbidden as well as the decay to on shell W and Z bosons,

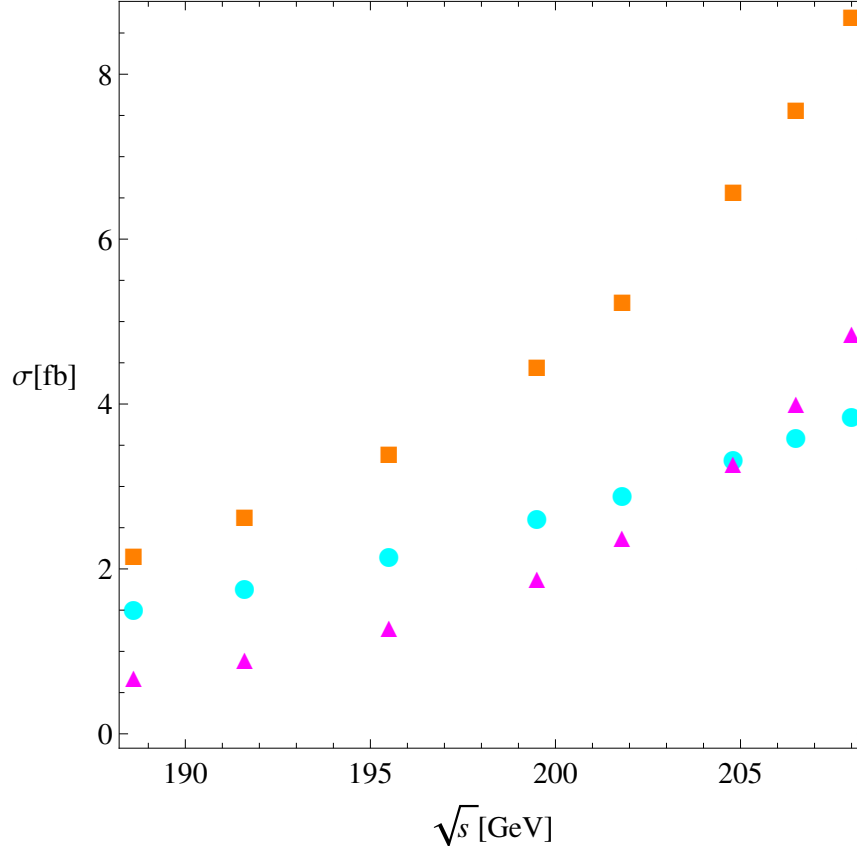


Figure 4: Cross sections for the Higgs production mechanism at LEP, Higgsstrahlung with an off-shell Z boson which decays to fermions (magenta triangle), vector boson fusion (sum of the process with W and Z bosons) including the inference with Higgsstrahlung (cyan circles) and the sum of these channels (orange rectangles) for $m_H = 125$ GeV.

\sqrt{s} [GeV]	$\sigma_{HS}[fb]$	$\sigma_{interference}[fb]$	$\sigma_{VBF}[fb]$	$\sigma_{total}[fb]$
188.6	$8.55 \cdot 10^{-2}$	0.4395	1.035	1.56
191.6	0.1056	0.5284	1.205	1.839
195.5	0.1392	0.6508	1.46	2.25
199.5	0.1895	0.8365	1.736	2.762
201.8	0.2291	0.9379	1.924	3.091
204.8	0.3041	1.1369	2.16	3.601
206.5	0.3634	1.2686	2.307	3.939
208.0	0.4349	1.4011	2.438	4.274

Table 4: The mean center of mass energy and the corresponding cross sections for the process $e^+e^- \rightarrow H\nu_e\nu_e$ at each experiment at LEP with $m_H = 125$ GeV. The numbers correspond to Fig. 5.

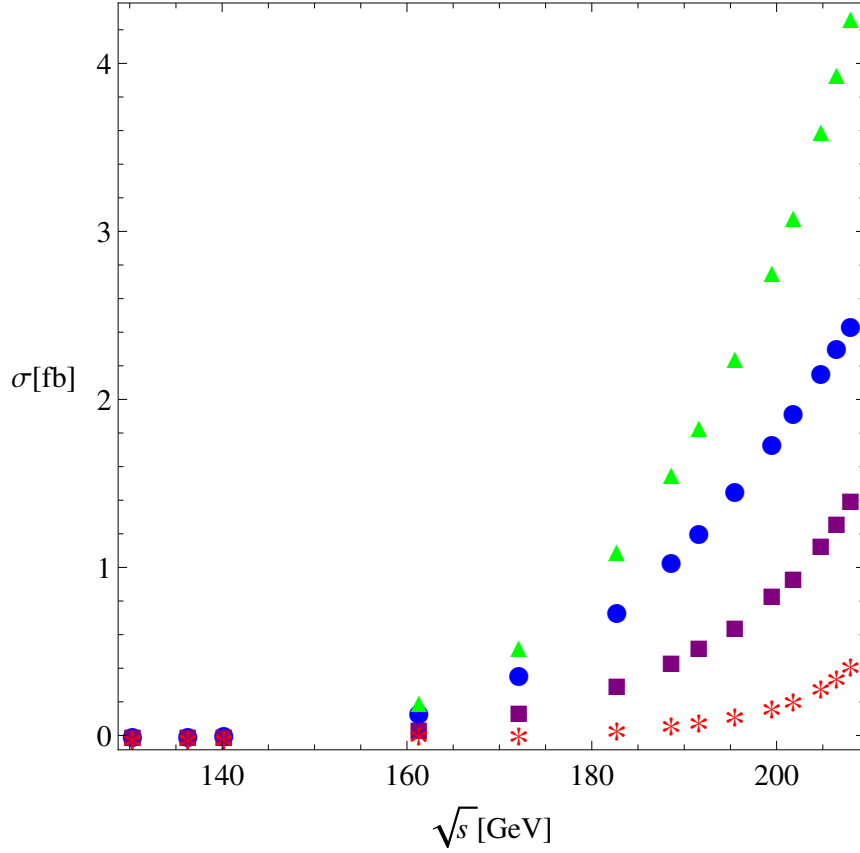


Figure 5: The cross sections for the process $e^+e^- \rightarrow H\bar{\nu}_e\nu_e$ (green triangle), W bosons fusion only (blue circles), the Z decay into electron neutrinos (red asterisk) and the interference term (purple rectangle) in dependence on the center of mass energy with $m_H = 125$ GeV.

\sqrt{s} [GeV]	$N_{VBF+interf}^{H\nu_e\bar{\nu}_e}$	$N_{VBF+interf}^{He^+e^-}$	N_{HS}	N_{total}
188.6	1.06164	0.0307944	0.500818	1.56246
191.6	0.208008	0.0055116	0.109825	0.317833
195.5	0.759888	0.0172224	0.46872	1.22861
199.5	0.9261	0.0170748	0.682812	1.60891
201.8	0.457904	0.0073088	0.382608	0.840512
204.8	1.05501	0.012032	1.05235	2.10736
206.5	1.85931	0.016	2.0864	3.94571
208.0	0.122851	0.0007904	0.155846	0.278698

Table 5: The number of events for Higgs production with vector boson fusion with W bosons including the interference term with Higgsstrahlung, vector boson fusion with Z bosons including the interference term from Higgsstrahlung with a subsequent decay of the Z boson to electrons and Higgsstrahlung where the Z boson decays to fermions for different center of mass energies at LEP for all 4 experiments with $m_H = 125$ GeV.

HS (with Z decay)		VBF+interf	total
m_H [GeV]	σ [fb]	σ [fb]	σ [fb]
115	59.3	7.015	66.315
125	3.808	3.6604	7.4684

Table 6: The cross sections for Higgs production processes (Higgsstrahlung and vector boson fusion including the interference term) as well as the total production cross section for $\sqrt{s} = 206.5$ GeV for $m_H = 115$ GeV and $m_H = 125$ GeV.

$BR(H \rightarrow f\bar{f})$				
m_H [GeV]	$c\bar{c}$	$b\bar{b}$	$\tau^+\tau^-$	gg
115	$3.27 \cdot 10^{-2}$	$7.05 \cdot 10^{-1}$	$7.65 \cdot 10^{-2}$	$8.76 \cdot 10^{-2}$
125	$2.68 \cdot 10^{-2}$	$5.78 \cdot 10^{-1}$	$6.37 \cdot 10^{-2}$	$8.56 \cdot 10^{-2}$

Table 7: The branching ratios for the decay of the Higgs boson to bottom or charm quarks, tau leptons or gluons [12].

so the largest branching ratio comes from the decay $H \rightarrow \bar{b}b$ with $BR = 5.78 \cdot 10^{-1}$ [12] (cf. Tab. 7) with $m_H = 125$ GeV. This channel was also used for the Higgs searches at LEP [4]. In Tab. 8 the number of events by using $N = \sigma_{H,prod} \cdot L \cdot BR(H \rightarrow f\bar{f})$ for the decays of an on shell Higgs boson into bottom quarks or tau leptons for different center of mass energies are summarised. For $\sigma_{H,prod}$ we take all production channels as discussed in the previous section into account.

The same calculations as above but for $m_H = 115$ GeV can be found in Tab. 9 with $BR(H \rightarrow \bar{b}b) = 7.05 \cdot 10^{-1}$ and $BR(H \rightarrow \tau\tau) = 7.65 \cdot 10^{-2}$ [12].

In the following we will focus on $\sqrt{s} = 206.5$ GeV and give estimates for expected number of Higgs events which would have been observed if LEP had run longer with this center of mass energy.

\sqrt{s} [GeV]	$N_{H \rightarrow bb}$	$N_{H \rightarrow \tau\tau}$
188.6	0.9031	0.0995285
191.6	0.183708	0.020246
195.5	0.710135	0.0782623
199.5	0.929951	0.102488
201.8	0.485816	0.0535406
204.8	1.21805	0.134239
206.5	2.28062	0.251342
208.0	0.161087	0.017753

Table 8: The mean center of mass energy and the expected number of events (at LEP for all four experiments) taking the decays of the Higgs boson ($m_H = 125$ GeV) into $\bar{b}b$ and $\tau\tau$ into account. For the Higgs production all possible channels as described in sec. 2.2 were used.

\sqrt{s} [GeV]	$N_{H,prod}$	$N_{H \rightarrow bb}$	$N_{H \rightarrow \tau\tau}$
188.6	3.75048	2.64409	0.286912
191.6	0.76992	0.542794	0.0588989
195.5	3.09312	2.18065	0.236624
199.5	4.554	3.21057	0.348381
201.8	2.728	1.92324	0.208692
204.8	10.6464	7.50571	0.81445
206.5	35.5524	25.0644	2.71976
208.0	3.5712	2.5177	0.273197

Table 9: The mean center of mass energy, the total number of produced Higgs bosons taking the processes described in sec. 2.2 into account and the number of Higgs bosons decaying into $b\bar{b}$ and $\tau^+\tau^-$ at LEP for $m_H = 115$ GeV.

Process	σ [pb] ($m_H = 115$ GeV)	σ [pb] ($m_H = 125$ GeV)
$e^+e^- \rightarrow H \rightarrow b\bar{b}q\bar{q}$	0.03729	0.003039
$e^+e^- \rightarrow H \rightarrow b\bar{b}\nu\bar{\nu}$	0.01631	0.00385
$e^+e^- \rightarrow H \rightarrow b\bar{b}l^+l^-$	0.003566	0.0003395
$e^+e^- \rightarrow H \rightarrow b\bar{b}\tau^+\tau^-$	0.001835	0.0001515
$e^+e^- \rightarrow H \rightarrow \tau^+\tau^-q\bar{q}$	0.001791	0.0001976
$e^+e^- \rightarrow H \rightarrow \tau^+\tau^-\nu\bar{\nu}$	0.0007849	0.000185

Table 10: The final states from the Higg production processes for $\sqrt{s} = 206.5$ GeV for $m_H = 115$ GeV and $m_H = 125$ GeV and the corresponding cross sections. For the final state including neutrinos or electrons also the Higgs production via vector boson has been included.

The experimental search at LEP focussed at the following final states

$$H \rightarrow b\bar{b}, Z \rightarrow q\bar{q}, H \rightarrow b\bar{b}, Z \rightarrow \nu\bar{\nu}, H \rightarrow b\bar{b}, Z \rightarrow l^+l^-, H \rightarrow \tau^+\tau^-, Z \rightarrow q\bar{q} \quad (2.4)$$

where also the contribution from vector boson fusion was taken into account. The corresponding cross sections for these final states are summarised in Tab. 10 where we include for completeness also the process $H \rightarrow \tau^+\tau^-, Z \rightarrow \nu\bar{\nu}$. For the final states including electrons or electron neutrinos vector boson fusion and the interference with Higgsstrahlung was also taken into account.

Summing up the cross sections for all processes and taking into account all four experiments at LEP and multiplying by the corresponding luminosity leads to ≈ 4 events at $\sqrt{s} = 206.5$ GeV for $m_H = 125$ GeV at LEP. If we assume that the luminosity was taken during a time of 6 months and that the luminosity in each additional year of operation at $\sqrt{s} = 206.5$ GeV at LEP is 800 pb^{-1} we would need ≈ 1.7 years to produce 50 Higgs bosons.

For $m_H = 115$ GeV the number of Higgs events is ≈ 32 which is about a factor of 8 larger than for a 125 GeV Higgs.

In order to discriminate the signal from the background one can use the reconstructed invariant mass distribution of the decay products of the Higgs boson and other variables. In Fig. 6 the distribution of the reconstructed Higgs boson mass with Monte Carlo predictions for signal and background events and the combined data from the experiments at LEP for $\sqrt{s} = 200 - 209$ GeV is shown. For the signal predictions a Higgs boson mass of 115 GeV

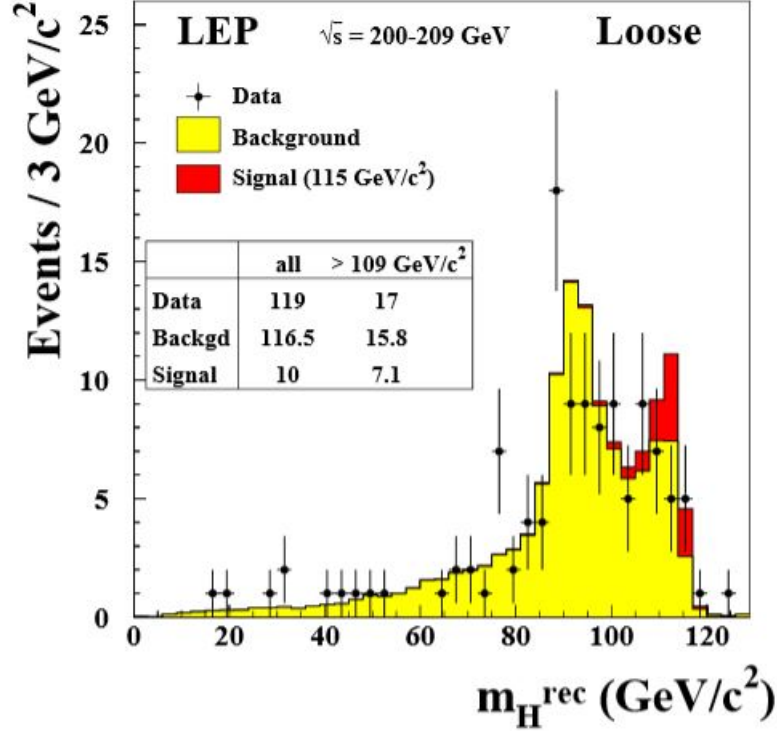


Figure 6: Distribution of the reconstructed Higgs boson mass m_H^{rec} taken from [4]. The yellow area shows the background prediction, the red area shows the prediction coming from Monte Carlo simulations for an assumed Standard Model Higgs boson of mass 115 GeV together with the data. In the loose selection the cuts are adjusted in such a way as to obtain, for a Higgs boson of mass 115 GeV approximately 0.5 or 2 times more expected signal than background events when integrated over the region $m_H^{rec} > 109$ GeV.

was assumed. The data shows one reconstructed Higgs boson with $m_H^{rec} = 125$ GeV but this data point is within its error bars compatible with zero Higgs events.

2.4 The effect of selection cuts, radiation and NLO corrections

To get an estimate for the actual possibility to observe Higgs bosons at LEP one has to consider the efficiency to select the right candidate events, ie. the effect of selection cuts. For the final state $H\nu\bar{\nu}$ with $m_H = 125$ GeV we use a efficiency to select the right candidate events of $\approx 60\%$ similar to the quoted efficiency for this channel for $m_H = 115$ GeV by DELPHI [13]. With this number we obtain ≈ 1.28 observable Higgs events at LEP for $\sqrt{s} = 206.5$ GeV and $m_H = 125$ GeV. For the channel $Hq\bar{q}$ we use an efficiency of $\approx 56\%$ to obtain ≈ 0.75 Higgs events at LEP. With the dominant production channel for a Higgs boson with $m_H = 115$ GeV ($H \rightarrow b\bar{b}$, $Z \rightarrow q\bar{q}$) we obtain ≈ 10.67 observable Higgs events.

The selection criteria for the Higgs events in the missing energy channel were for example at OPAL [14] that the visible energy has to be less than 80% of \sqrt{s} , the total visible p_T has to be larger than 3 GeV, the visible mass has to be larger than 4 GeV and the missing mass between 50 and 130 GeV and other criteria concerning the geometry to further reduce the background. For the channel $b\bar{b}\nu\bar{\nu}$ the cross section for $m_H = 125$ GeV and $\sqrt{s} = 206.5$ GeV

is $\sigma = 0.003932$ pb, cf. Tab. 10. Imposing these cuts the cross section decreases by 20% to $\sigma = 0.003124$ pb. Also for $m_H = 115$ GeV the cross section shrinks from $\sigma = 0.01668$ pb to $\sigma = 0.01587$ pb which is a change of 4%.

Removing all the other constraints except for the upper limit on the missing mass we get the uncut cross section back. The cuts have more effect on a Higgs boson with $m_H = 125$ GeV than on a 115 GeV Higgs boson, probably because the analyses concentrated at m_H below 120 GeV [13–16] where the Z boson in the Higgs production process via Higgsstrahlung could be on shell. The same cut on the mass recoiling against the hadronic system (the invisible mass) was also imposed by the L3 collaboration [15].

Coming now to the effects of initial and final state radiation: In Fig. 7 the signal and the background for $e^+e^- \rightarrow \nu\bar{\nu}b\bar{b}$ are shown for $\sqrt{s} = 206.5$ GeV without imposing selection cuts and with and without taking initial and final state radiation into account. The luminosity is $L = 130$ pb $^{-1}$ which corresponds to one experiment at LEP. The simulation of the events was done with MadGraph and for the jet clustering the FastJet package was used where the jet algorithm is antikt, the minimum p_T is 5 GeV and the jet radius parameter is fixed to $R=1$. The Monte Carlo predictions show signal events around an invariant mass of the decay products around 125 GeV in Fig. 7. Hence by analysing the invariant mass distribution of the b quarks the signal events can be distinguished from the background although the total number of background events is 20 times larger than the number of signal events.

As it can be seen in Fig. 8 radiation shifts the distribution to smaller values of the invariant mass of the b quark pair. The distribution of number of events where only initial or final state radiation is taken into account can be found in App. B.

Fig. 9 shows the missing transverse energy in this process without taking radiation into account. Taking initial or final state radiation into account does not change the distribution because the missing transverse energy comes from the neutrinos which are unaffected by radiation.

Changing the R parameter of the jet algorithm to $R=0.3$ the distribution from Fig. 7 changes as it can be seen in Fig. 10. The distribution is more smeared out as with $R=1$ which can be understood since the R parameter defines the radius between the particles which are clustered together as a jet. This smearing reduces the ability to distinguish signal from background events and hence the optimal choice for the right R parameter is important in the analysis.

In App. B a more detailed analysis of the effect of a smaller R parameter is presented.

Turning now to the final state involving tau leptons. In Fig. 11 the number of signal and background events for $e^+e^- \rightarrow \nu\bar{\nu}\tau^+\tau^-$ is represented. The jets originating from the decaying tau leptons are reconstructed as non-b tagged jets. The signal is nearly invisible on the large background. Which can be understood since the total number of background events exceeds the number of signal events by a factor of 1300. In Fig. 12 the number of signal+background events with initial and final state radiation is compared to the number of signal+background events without radiation is compared. We see that the effect of radiation is smaller compared to its effect on the final state with the b quarks since there also QCD plays a role which is not possible for the leptons.

The distribution of the missing energy is represented in Fig. 13. Further figures for the final state including tau leptons can be found in App. B.

Coming to NLO corrections in the processes: QCD corrections are more important than electroweak corrections. Especially for the final state with b jets, ie. the decay of the Higgs boson to quarks, gets rather large QCD corrections. For example the partial width $\Gamma_{H \rightarrow b\bar{b}}$

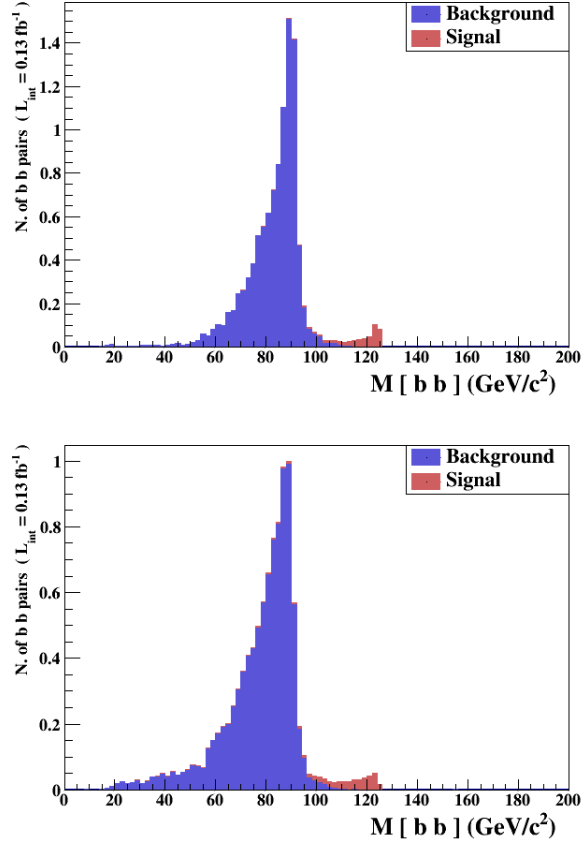


Figure 7: The number of signal and background events for $e^+e^- \rightarrow \nu\bar{\nu}b\bar{b}$, $m_H = 125$ GeV and $\sqrt{s} = 206.5$ GeV. The blue areas show the prediction for the background only, the red areas show the signal prediction from a MadGraph. The upper plot shows the number of events without radiation, the lower one shows the number of events with initial and final state radiation for the b quark pair.

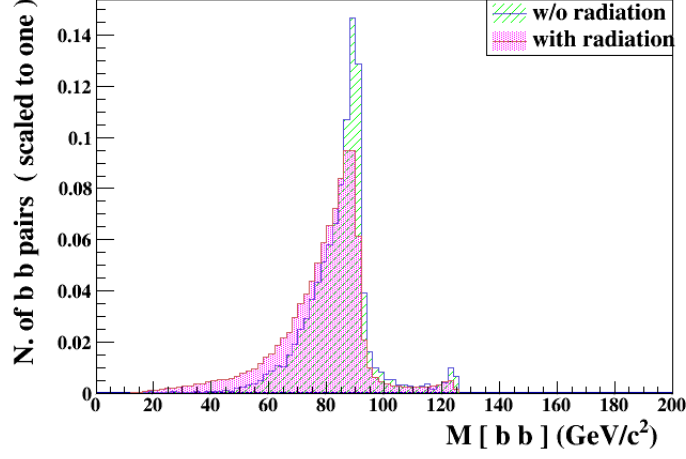


Figure 8: Comparison of the number of signal+background events for $e^+e^- \rightarrow \nu\bar{\nu}b\bar{b}$ and $\sqrt{s} = 206.5$ GeV and $m_H = 125$ GeV. The green area shows the prediction for the signal+background events without radiation, the pink area shows the signal+background events with initial and final state radiation.

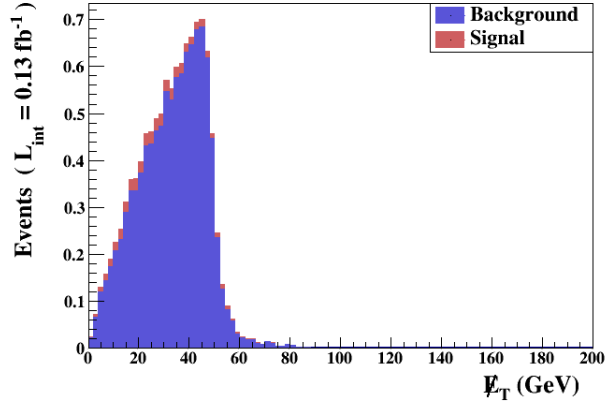


Figure 9: The missing transverse energy of signal and background events for $e^+e^- \rightarrow \nu\bar{\nu}b\bar{b}$ and $\sqrt{s} = 206.5$ GeV without taking radiation into account. The blue area shows the prediction for the background only, the red area shows the signal prediction from a MadGraph.

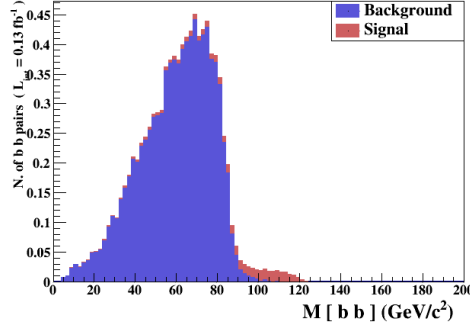


Figure 10: The number of signal and background events for $e^+e^- \rightarrow \nu\bar{\nu}b\bar{b}$ and $\sqrt{s} = 206.5$ GeV. The blue area shows the prediction for the background only, the red area shows the signal prediction from a MadGraph. The plots show the number of events with initial and final state radiation for invariant mass of b tagged jets with $R=0.3$.

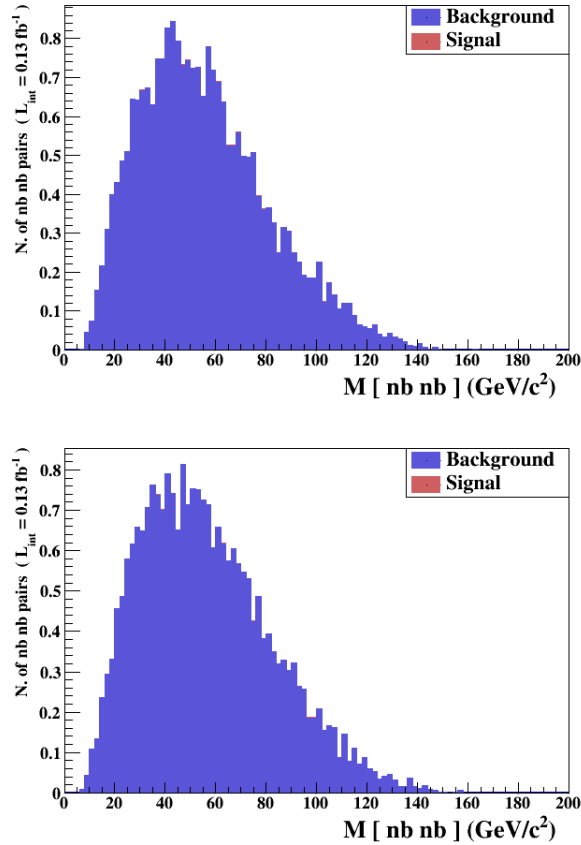


Figure 11: The number of signal and background events for $e^+e^- \rightarrow \nu\bar{\nu}\tau^+\tau^-$ and $\sqrt{s} = 206.5$ GeV, $m_H = 125$ GeV. The blue areas show the prediction for the background only, the red areas show the signal prediction from a MadGraph. The plots show (from top to bottom) the number of events without radiation, with initial state radiation, with final state radiation and with initial and final state radiation for the tau lepton pair.

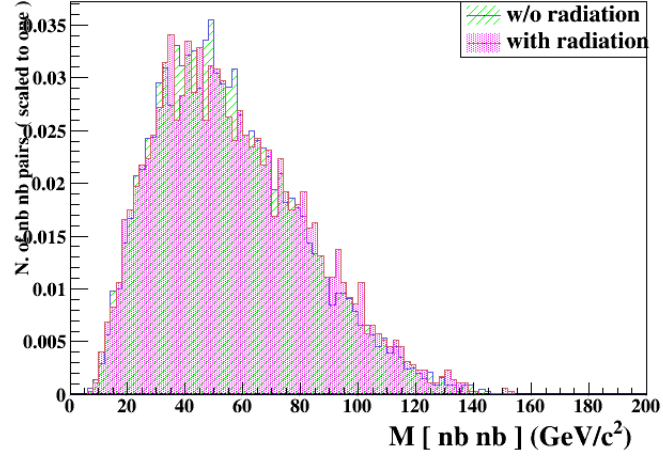


Figure 12: Comparison of the number of signal+background events for $e^+e^- \rightarrow \nu_l \bar{\nu}_l \tau^+ \tau^-$ and $\sqrt{s} = 206.5$ GeV. The green area shows the prediction for the signal+background events without radiation, the pink area shows the signal+background events with initial and final state radiation.

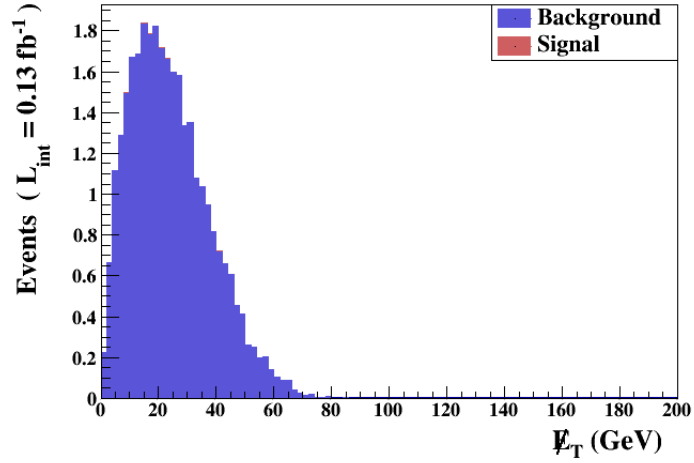


Figure 13: The missing transverse energy for the signal events (red) and the background events (blue) for $e^+e^- \rightarrow \nu_l \bar{\nu}_l \tau^+ \tau^-$ and $\sqrt{s} = 206.5$ GeV, $m_H = 125$ GeV.

gets a correction of 20% [17] which can be absorbed using the running b quark mass which changes from $m_b(m_b) = 4.18$ GeV to $m_b(m_H) = 2.82$ GeV [3].

3 Coupling of the Higgs boson to the Z boson

At LEP 95% CL limits on the coupling of the Higgs boson to the Z boson for different values of the Higgs mass were obtained, see Fig. 2. In Beyond-the-Standard-Model (BSM) theories like Supersymmetry (SUSY) the coupling of the Higgs boson to the gauge bosons gets modified. The cross section for the production of the light CP-even scalar Higgs boson in SUSY with Higgsstrahlung at lepton colliders (ie. the process $e^+e^- \rightarrow h^0 Z$) differs from the Standard Model prediction by a factor $\sin^2(\alpha - \beta)$ [11]. The model parameter α describes the mixing of the two CP-even Higgs mass eigenstates h_0, H_0 and $\tan \beta = v_u/v_d$ is the ratio of the VEVs of the up-type and down-type Higgs doublet. At future lepton colliders like ILC or CLIC with higher luminosity and higher energy improved limits of the HZZ coupling can be obtained which can be used to probe the parameter space of BSM models.

The analysis of the coupling is based on a modified frequentist approach where the logarithm of the ratio of the likelihood functions for the signal-plus-background hypothesis and the background-only hypothesis is used as a statistical estimator. This is defined as

$$-2\ln Q = 2s_{tot} - 2 \sum_i n_i \ln \left(1 + \frac{s_i}{b_i} \right), \quad (3.1)$$

where i runs over the number of bins of the distribution of the discriminating observable we define and n_i, s_i, b_i are the number of observed, expected signal and expected background events in the bin. We define $s_{tot} = \sum_i s_i$ as the total expected number of signals. A negative value of $-2\ln Q$ shows preference for signal+background events. With an increasing luminosity also the number of observed events (background and signal+background, if there is a signal) increases as well as the statistical preference for the observable.

4 Summary and Conclusion

In this summer student report we have investigated the expected signal and background events for a SM-like Higgs boson at LEP. There are two dominant production mechanisms for a 125 GeV Higgs Boson at LEP with energies around 200 GeV. One is the vector boson fusion with an important (around 30%) contribution from the Higgsstrahlung coming from the subsequent decay of the Z boson to electron neutrinos. The other production channel is Higgsstrahlung with a subsequent decay of the Z boson to a fermion-antifermion pair.

The dominant decay channels of a 125 GeV Higgs boson is the decay to b quarks. Taking all possible final states arising from Higgs boson production processes where the Higgs decays either to b quarks or to tau leptons into account, the expected number of Higgs events is ≈ 4 at LEP with $\sqrt{s} = 206.5$ GeV and $L = 520$ pb $^{-1}$. It turns out that the signal in the process $e^+e^- \rightarrow b\bar{b}\nu\bar{\nu}$ can be distinguished from the background by an analysis of the invariant mass distribution of the b jets whereas the background dominates for the process $e^+e^- \rightarrow \tau^+\tau^-\nu_l\bar{\nu}_l$.

The effect of initial and final state radiation is more important for the final state involving b jets than tau leptons since for the b jets also QCD radiation is possible. Radiation leads to smaller invariant masses of the b jets in the process.

Changing the jet radius parameter R to smaller values (from 1 to 0.3) leads to a smearing of the invariant mass distribution of the b quarks and hence lower the ability to distinguish signal events from background events.

NLO corrections are expected to play a minor role in the analysis and are not considered.

The limits of the HZZ coupling are important to restrict the parameter space of BSM theories and these could be improved at future lepton colliders with higher luminosity and higher energy.

Acknowledgment

I would like to thank my supervisors Emanuele Bagnaschi and Georg Weiglein for their support and useful discussions during my stay at DESY and for providing me this interesting topic.

Furthermore I would like to thank the coordinators of the summer student programme and especially the other summer students for making my stay at Hamburg a very pleasant experience.

References

- [1] S. Chatrchyan *et al.* [CMS Collaboration], Phys. Lett. B **716** (2012) 30 [arXiv:1207.7235 [hep-ex]].
- [2] G. Aad *et al.* [ATLAS Collaboration], Phys. Lett. B **716** (2012) 1 [arXiv:1207.7214 [hep-ex]].
- [3] K.A. Olive *et al.* (Particle Data Group), Chin. Phys. C, **38**, 090001 (2014).
- [4] R. Barate *et al.* [LEP Working Group for Higgs boson searches and ALEPH and DELPHI and L3 and OPAL Collaborations], Phys. Lett. B **565** (2003) 61 [hep-ex/0306033].
- [5] S. Schael *et al.* [ALEPH and DELPHI and L3 and OPAL and SLD and LEP Electroweak Working Group and SLD Electroweak Group and SLD Heavy Flavour Group Collaborations], Phys. Rept. **427** (2006) 257 [hep-ex/0509008].
- [6] J. A. Aguilar-Saavedra *et al.* [ECFA/DESY LC Physics Working Group Collaboration], hep-ph/0106315.
- [7] W. Kilian, M. Kramer and P. M. Zerwas, Phys. Lett. B **373** (1996) 135 [hep-ph/9512355].
- [8] M. Carena and H. E. Haber, Prog. Part. Nucl. Phys. **50** (2003) 63 [hep-ph/0208209].
- [9] J. Alwall *et al.*, JHEP **1407** (2014) 079 [arXiv:1405.0301 [hep-ph]].
- [10] S. Schael *et al.* [ALEPH and DELPHI and L3 and OPAL and LEP Electroweak Collaborations], Phys. Rept. **532** (2013) 119 [arXiv:1302.3415 [hep-ex]].
- [11] M. M. Kado and C. G. Tully, Ann. Rev. Nucl. Part. Sci. **52** (2002) 65.
- [12] S. Dittmaier *et al.* [LHC Higgs Cross Section Working Group Collaboration], arXiv:1101.0593 [hep-ph].

- [13] J. Abdallah *et al.* [DELPHI Collaboration], Eur. Phys. J. C **32** (2004) 145 [hep-ex/0303013].
- [14] G. Abbiendi *et al.* [OPAL Collaboration], Eur. Phys. J. C **26** (2003) 479 [hep-ex/0209078].
- [15] P. Achard *et al.* [L3 Collaboration], Phys. Lett. B **517** (2001) 319 [hep-ex/0107054].
- [16] A. Heister *et al.* [ALEPH Collaboration], Phys. Lett. B **526** (2002) 191 [hep-ex/0201014].
- [17] A. Djouadi, Phys. Rept. **457** (2008) 1 [hep-ph/0503172].

A The diagrams for the background processes

The diagrams for the background processes for $e^+e^- \rightarrow b\bar{b}\nu\bar{\nu}$ can be found in Figs. (14,15) and for $e^+e^- \rightarrow \tau^+\tau^-\nu\bar{\nu}$ in Figs. (16,17,18).

B Detailed plots concerning the effect of radiation and the change of the R-parameter

In this appendix more plots for the number of events in the channels $e^+e^- \rightarrow \nu\bar{\nu}b\bar{b}$ and $e^+e^- \rightarrow \nu\bar{\nu}\tau^+\tau^-$ showing the effect of radiation and change of the jet radius parameter are given.

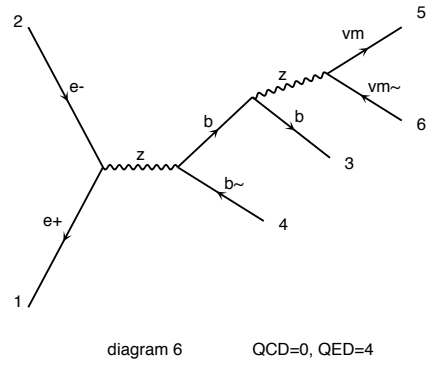
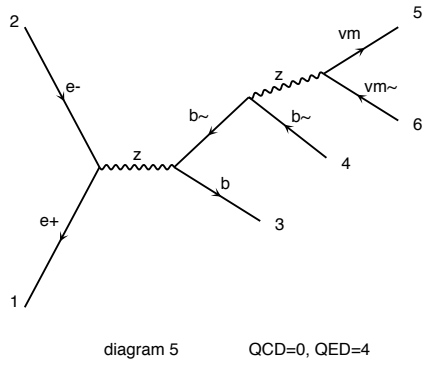
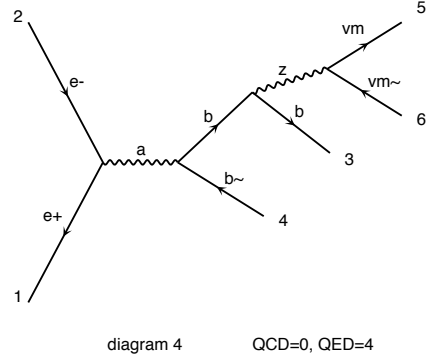
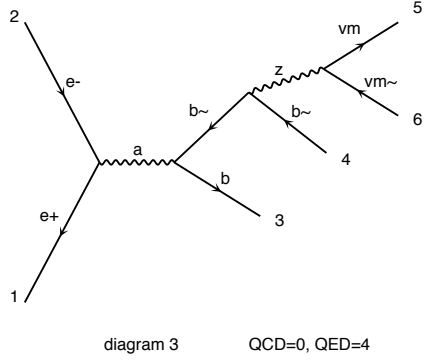
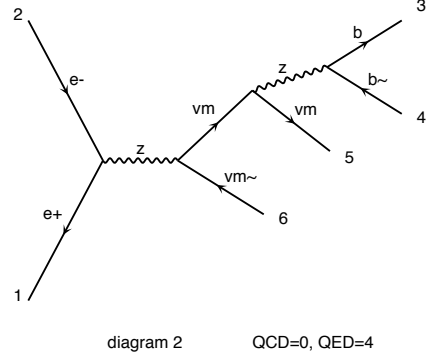
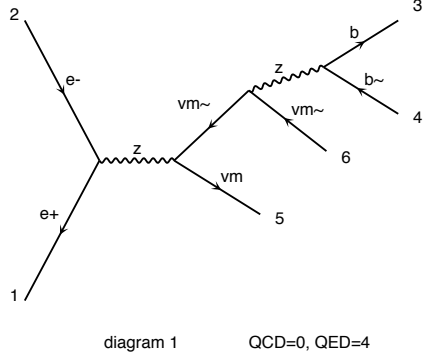
In Fig. 19 the number of events in the channel $e^+e^- \rightarrow \nu_l\bar{\nu}_l b\bar{b}$, $m_H = 125$ GeV and $\sqrt{s} = 206.5$ GeV taking initial or final state radiation into account are represented. Furthermore in Fig. 20 the number of events including initial and final state radiation for different combination of b tagged (b), non-b tagged (nb) and jets (non-b tagged and b tagged jets) are shown.

The number of jets for signal and background events for $\sqrt{s} = 206.5$ GeV with initial and final state radiation is represented in Fig. 21. The number of non-b jets is nearly two times larger than the number of b-tagged jets. We also see that the number of non-b tagged jets emerging from signal events is very close to zero.

Changing the jet radius parameter from $R=1$ to $R=0.3$ leads to a smaller number of tracks as can be seen in Fig.22 where the number of tracks for events with initial and final state radiation are shown in comparison with $R=0.3$ and $R=1$. Also the number of jets is affected by the change of R as it can be seen in Fig. 23. The number of jets is smaller compared to Fig. 21. The distribution for the number of events (Fig. 24) also changes in comparison to Fig. 20

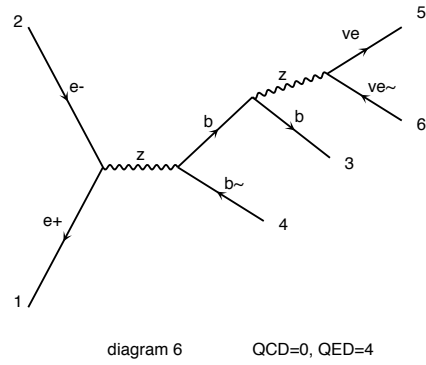
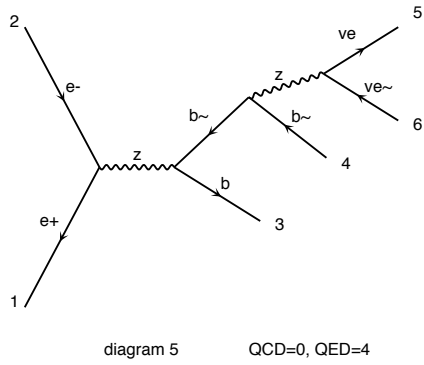
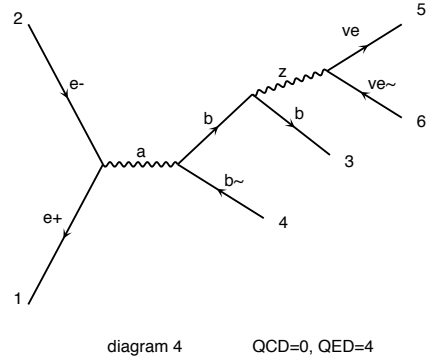
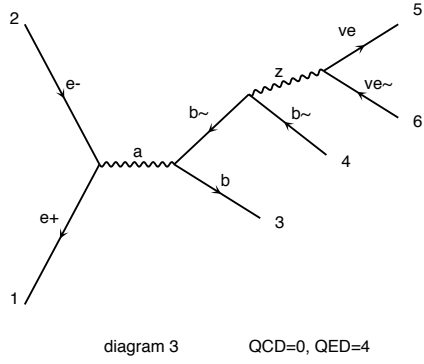
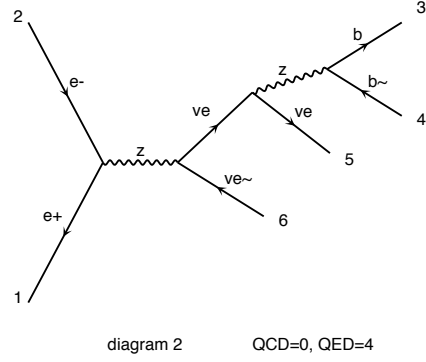
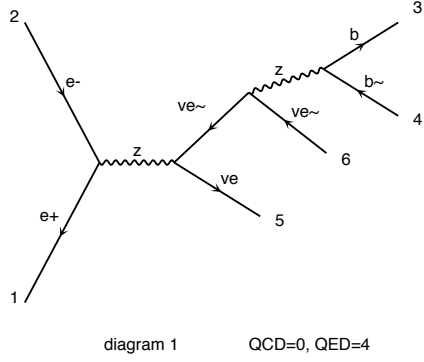
Turning now to the final state involving tau leptons.

In Fig. 25 the number of events in dependence on the invariant mass for two tau jets taking initial or final state radiation into account and in Fig. 26 the number of events of three jets for processes involving final and initial state radiation is shown.



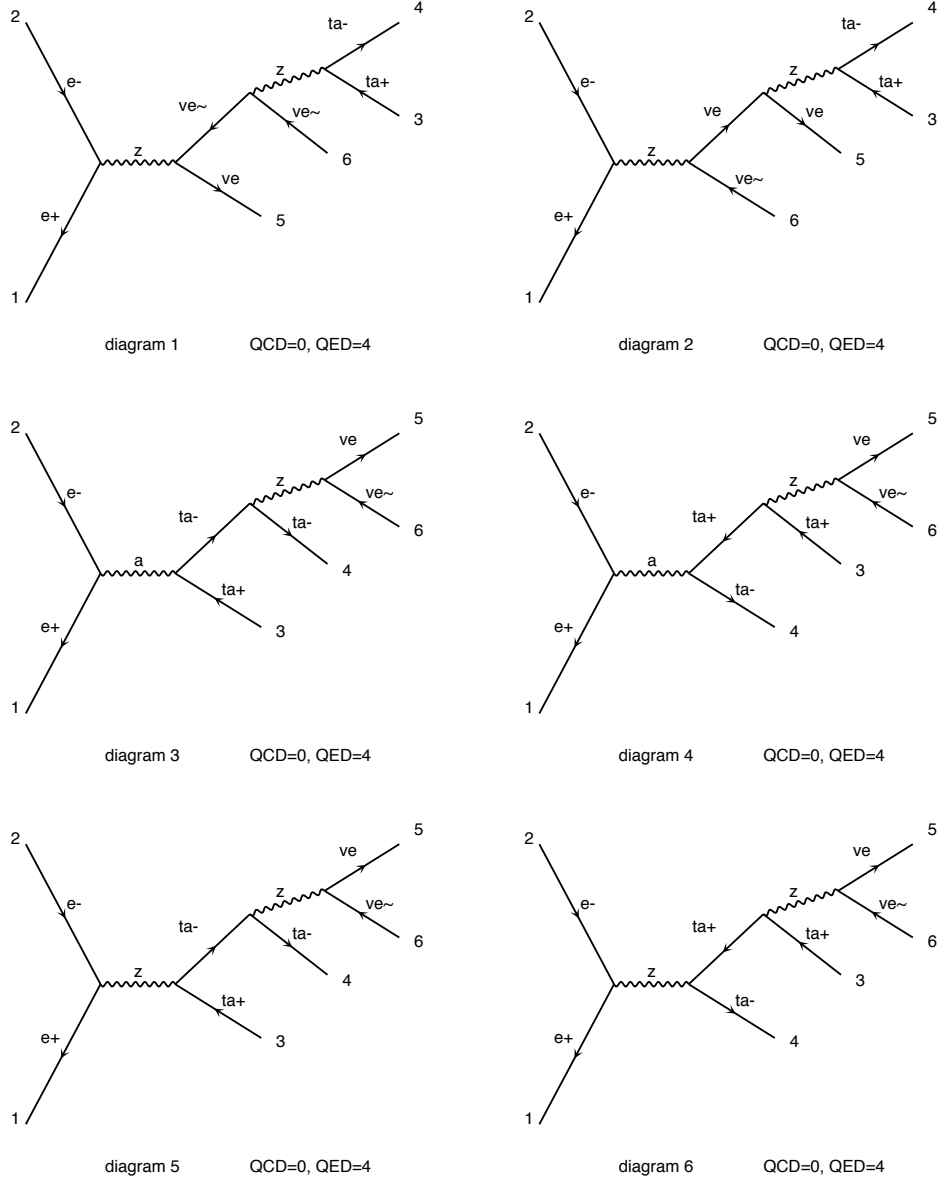
Diagrams made by MadGraph5_aMC@NLO

Figure 14: Background processes for $e^+e^- \rightarrow b\bar{b}\nu_l\bar{\nu}_l$.



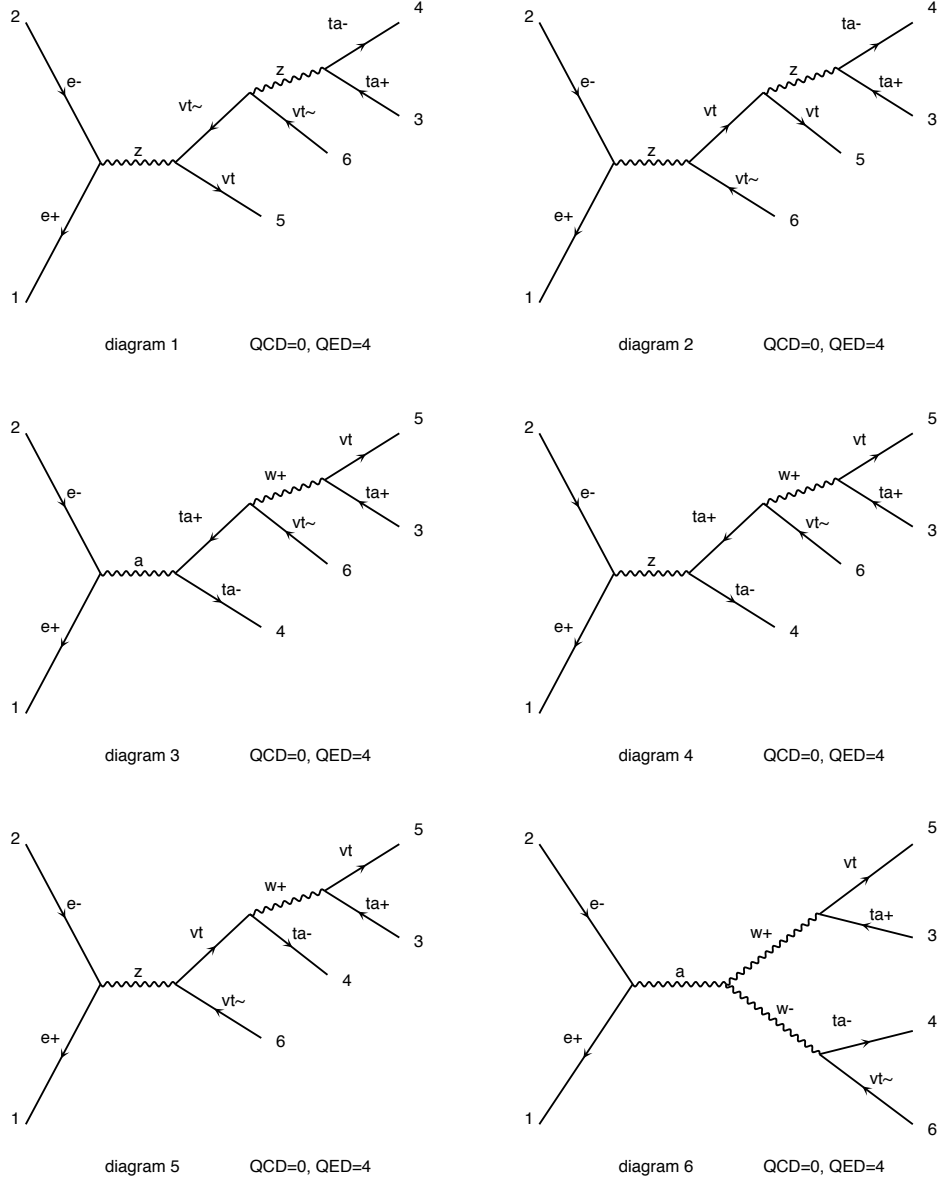
Diagrams made by MadGraph5_aMC@NLO

Figure 15: Background processes for $e^+e^- \rightarrow b\bar{b}\nu_l\bar{\nu}_l$.



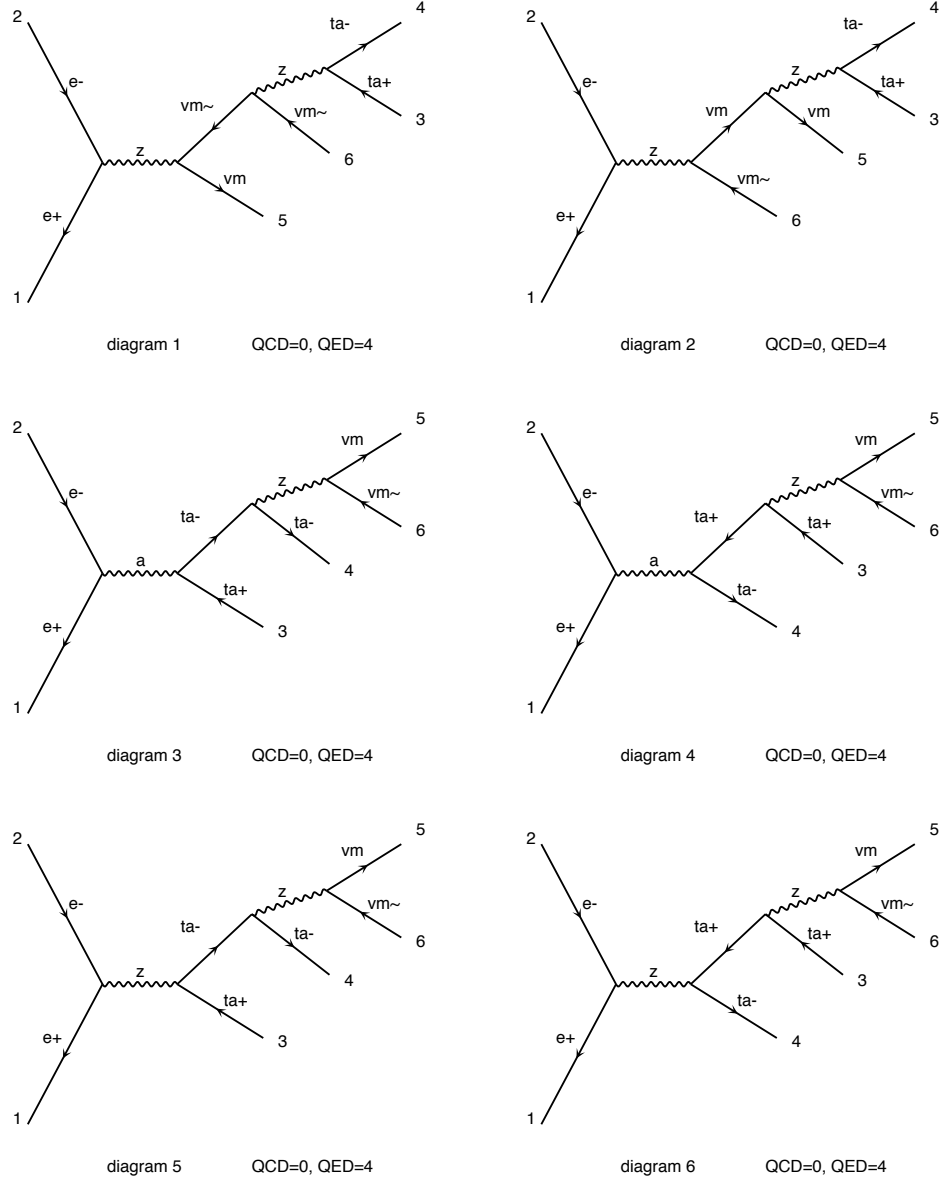
Diagrams made by MadGraph5_aMC@NLO

Figure 16: Background processes for $e^+e^- \rightarrow \tau^+\tau^-\nu_l\bar{\nu}_l$.



Diagrams made by MadGraph5_aMC@NLO

Figure 17: Background processes for $e^+e^- \rightarrow \tau^+\tau^-\nu_l\bar{\nu}_l$.



Diagrams made by MadGraph5_aMC@NLO

Figure 18: Background processes for $e^+e^- \rightarrow \tau^+\tau^-\nu_l\bar{\nu}_l$.

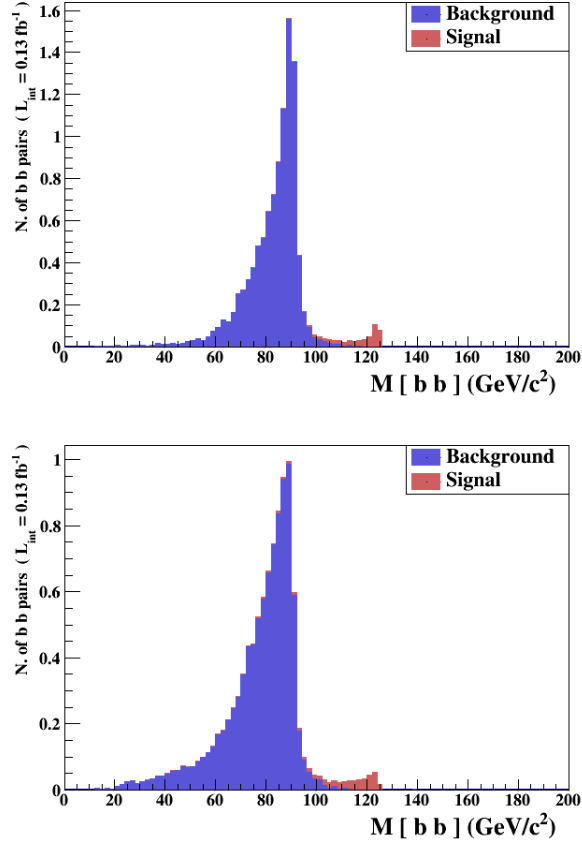


Figure 19: The number of signal and background events for $e^+e^- \rightarrow \nu\bar{\nu}b\bar{b}$, $m_H = 125$ GeV and $\sqrt{s} = 206.5$ GeV. The blue areas show the prediction for the background only, the red areas show the signal prediction from a MadGraph. The upper plot shows the number of events with initial state radiation, the lower one with final state radiation in dependence on the invariant mass of the b quark pair.

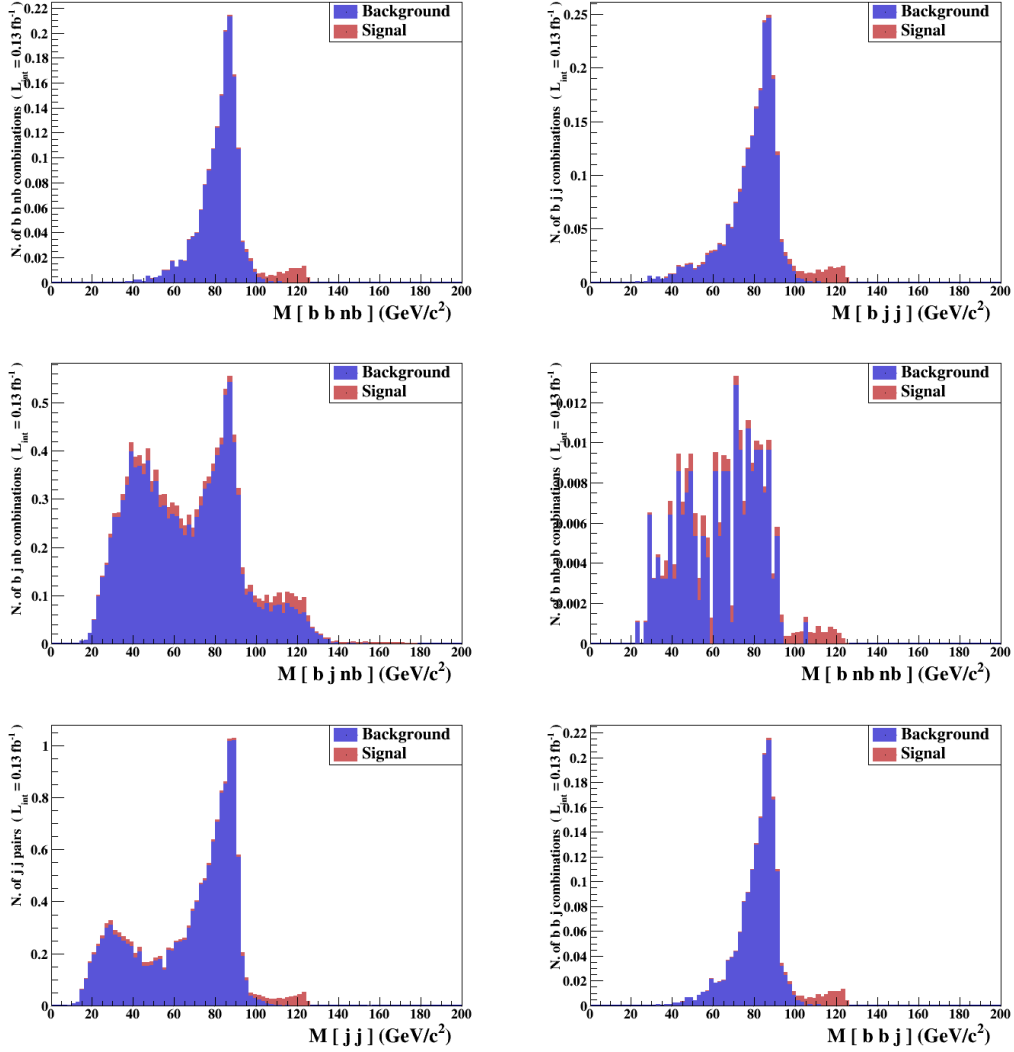


Figure 20: The number of signal and background events for $e^+e^- \rightarrow \nu\bar{\nu}b\bar{b}$, $m_H = 125$ GeV and $\sqrt{s} = 206.5$ GeV. The blue areas show the prediction for the background only, the red areas show the signal prediction from a MadGraph. The plots show the number of events with initial and final state radiation for invariant mass of b tagged (b), non b tagged (nb) jets and jets (non b tagged and b tagged) where the R-parameter of the jet algorithm is fixed to 1.

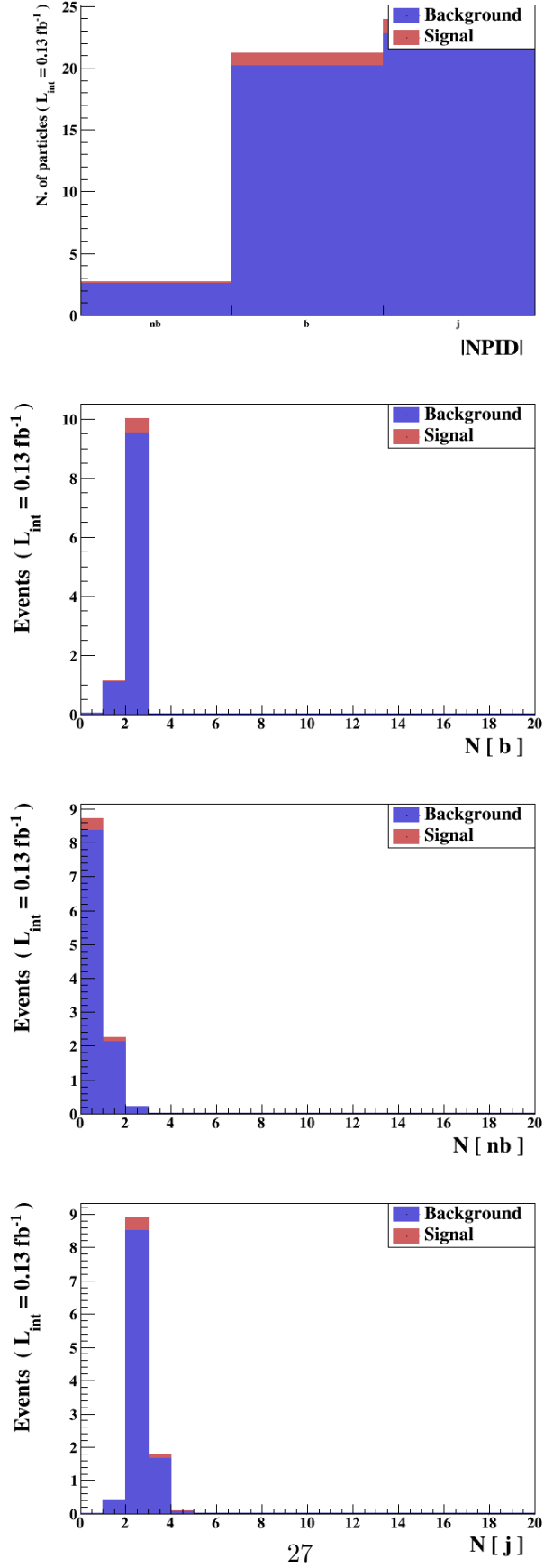


Figure 21: The number of jets for signal and background events for $e^+e^- \rightarrow \nu\bar{\nu}b\bar{b}$, $m_H = 125$ GeV and $\sqrt{s} = 206.5$ GeV with initial and final state radiation. The blue areas show the prediction for the background only, the red areas show the signal prediction from a MadGraph.

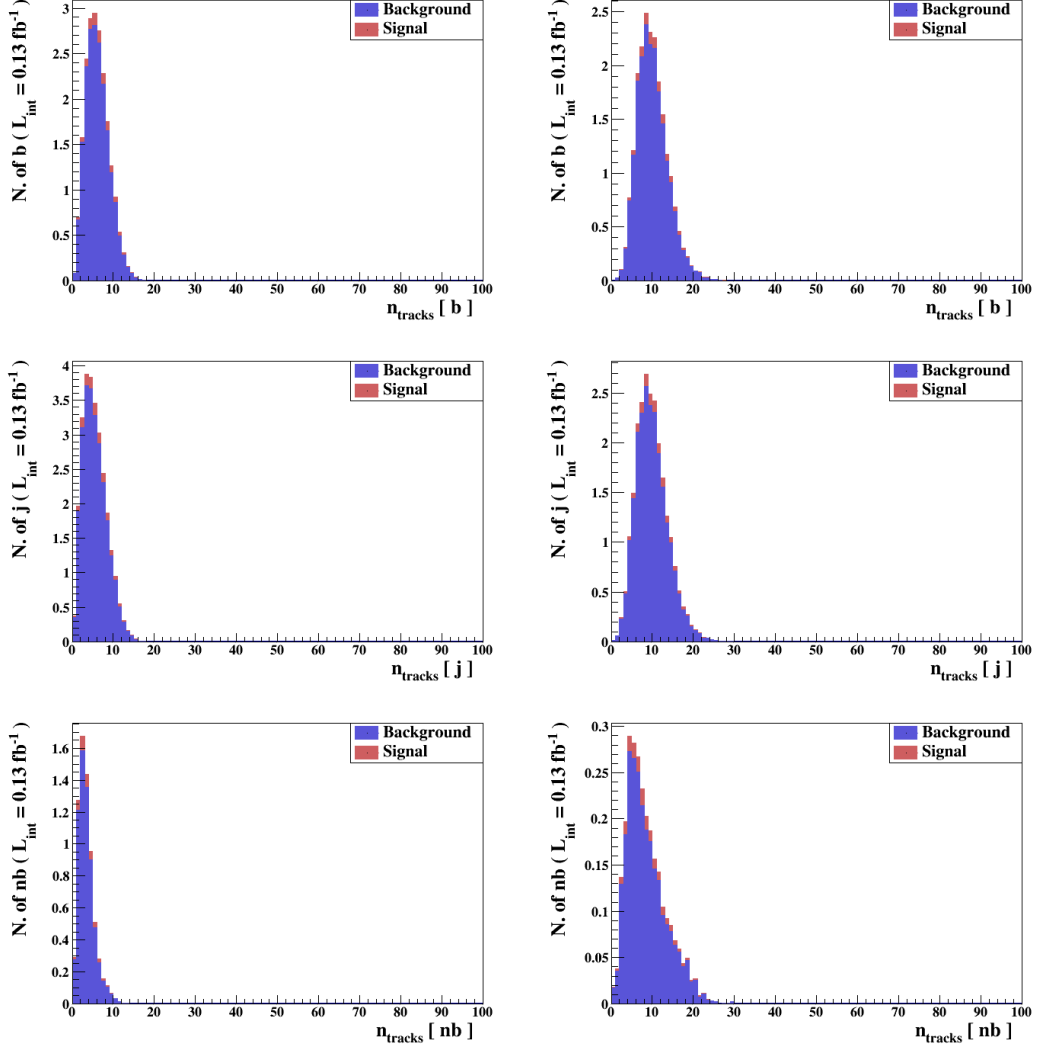


Figure 22: The number of tracks of signal and background events for $e^+e^- \rightarrow \nu\bar{\nu}b\bar{b}$ and $\sqrt{s} = 206.5$ GeV. The blue areas show the prediction for the background only, the red areas show the signal prediction from a MadGraph. The plots show the events with initial and final state radiation for $R=0.3$ (left plots) and $R=1$ (right plots).

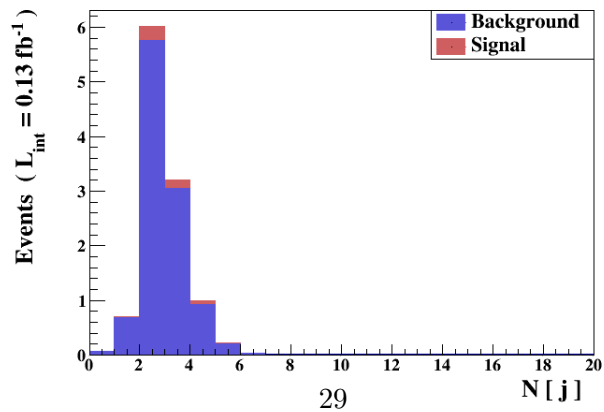
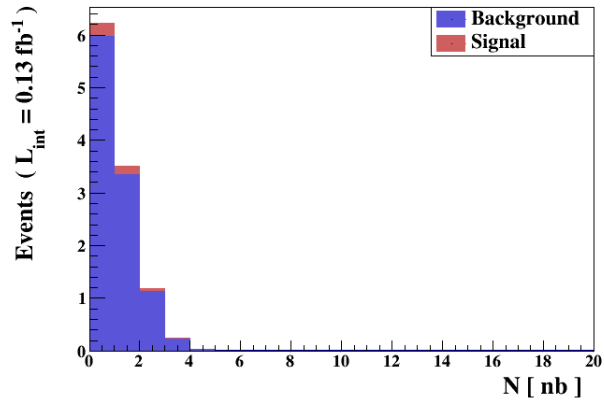
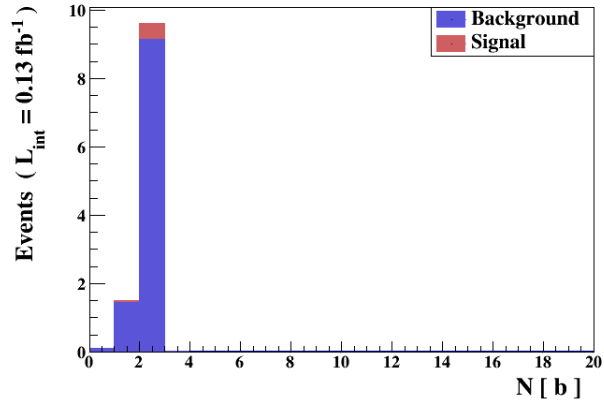
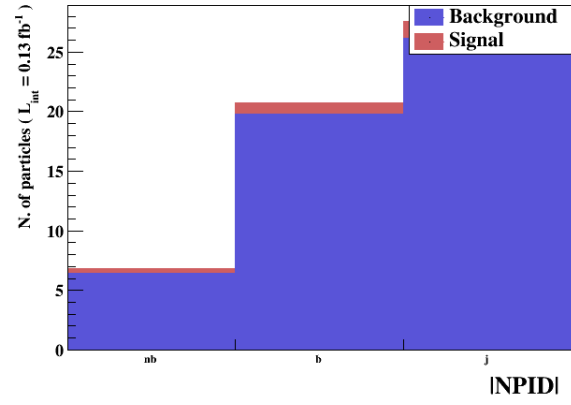


Figure 23: The number of jets for signal (red) and background (blue) events for $e^+e^- \rightarrow \nu\bar{\nu}b\bar{b}$, $m_H = 125$ GeV and $\sqrt{s} = 206.5$ GeV with initial and final state radiation with $R=0.3$.

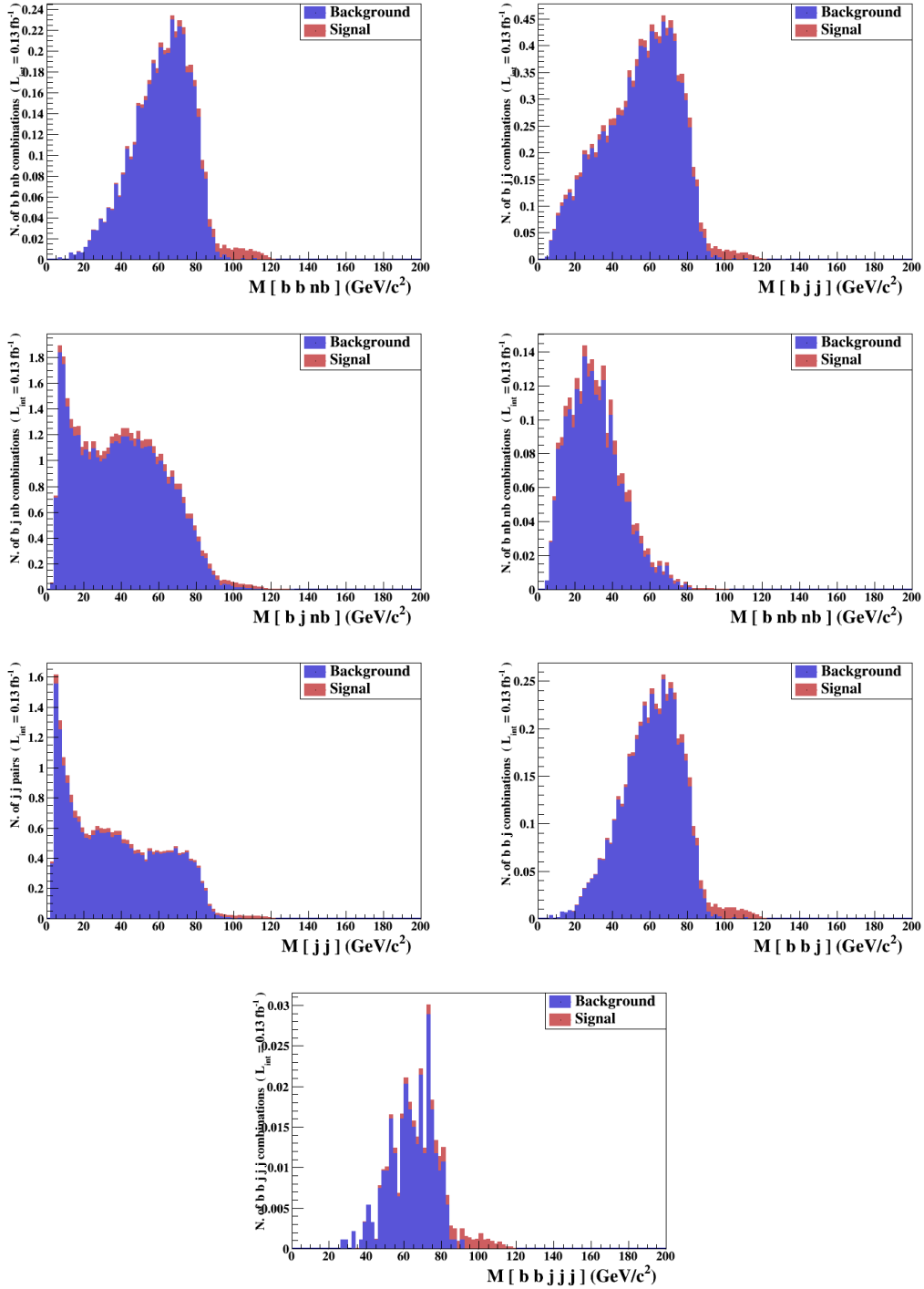


Figure 24: The number of signal and background events for $e^+e^- \rightarrow \nu\bar{\nu}b\bar{b}$ and $\sqrt{s} = 206.5$ GeV. The blue areas show the prediction for the background only, the red areas show the signal prediction from a MadGraph. The plots show the number of events with initial and final state radiation for invariant mass of b tagged, non-b tagged (nb) jets and jets in general with $R=0.3$.

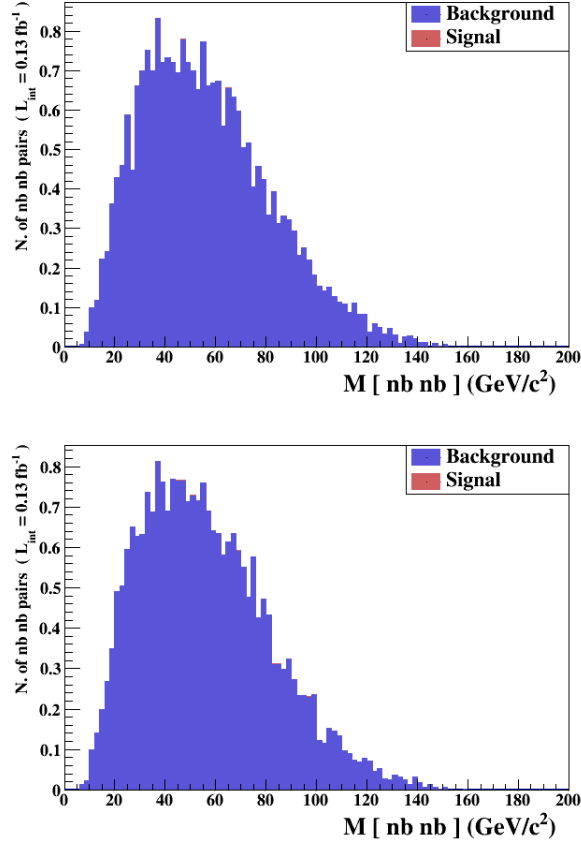


Figure 25: The number of signal and background events for $e^+e^- \rightarrow \nu\bar{\nu}\tau^+\tau^-$ and $\sqrt{s} = 206.5$ GeV, $m_H = 125$ GeV. The blue areas show the prediction for the background only, the red areas show the signal prediction from a MadGraph. The upper plot shows the number of events with initial state radiation, the lower plot with final state radiation for the tau lepton pair.

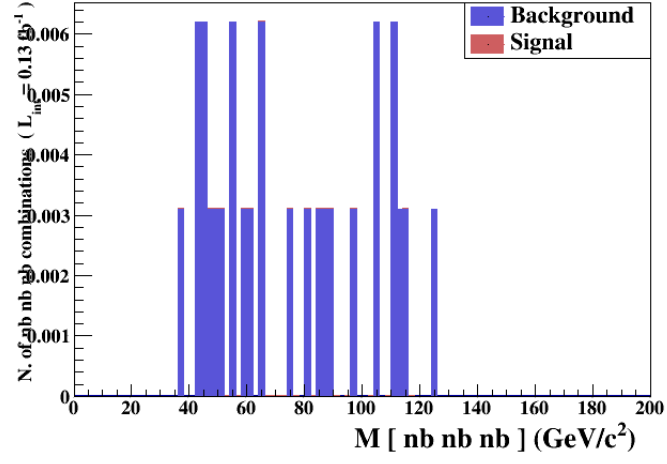


Figure 26: Comparison of the number of signal+background events for $e^+e^- \rightarrow \nu\bar{\nu}s\tau^+\tau^-$ and $\sqrt{s} = 206.5$ GeV. The blue areas show the prediction for the background only, the red areas show the signal prediction from a MadGraph. The plot shows the number of events in dependence of the invariant mass of three jets for background and signal processes with initial and final state radiation.